

## Interleukin-33 overexpression is associated with liver fibrosis in mice and humans

Pierrick Marvie<sup>a</sup>, Mariette Lisbonne<sup>a</sup>, Annie L'Helgoualc'h<sup>a</sup>, Michel Rauch<sup>a</sup>, Bruno Turlin<sup>b</sup>, Laurence Preisser<sup>c</sup>, Katia Bourd-Boittin<sup>a</sup>, Nathalie Théret<sup>a</sup>, Hugues Gascan<sup>c</sup>, Claire Piquet-Pellorce<sup>a</sup>, Michel Samson<sup>a,\*</sup>

<sup>a</sup> EA 4427 SeRAIC-U.620 INSERM, Université de Rennes 1, Rennes, France

<sup>b</sup> Service d'Anatomo-pathologie, CHU Pontchaillou, Rennes, France

<sup>c</sup> INSERM U564, Angers, France

Received: February 18, 2009; Accepted: May 5, 2009

### Abstract

Interleukin-33 (IL-33), the most recently identified member of the IL-1 family, induces synthesis of T Helper 2 (Th2)-type cytokines *via* its heterodimeric ST2/IL-1RAcP receptor. Th2-type cytokines play an important role in fibrosis; thus, we investigated the role of IL-33 in liver fibrosis. IL-33, ST2 and IL-1RAcP gene expression was analysed in mouse and human normal ( $n = 6$ ) and fibrotic livers ( $n = 28$ ), and in human hepatocellular carcinoma (HCC;  $n = 22$ ), using real-time PCR. IL-33 protein was detected in normal and fibrotic liver sections and in isolated liver cells using Western blotting and immunolocalization approaches. Our results showed that IL-33 and ST2 mRNA was overproduced in mouse and human fibrotic livers, but not in human HCC. IL-33 expression correlated with ST2 expression and also with collagen expression in fibrotic livers. The major sources of IL-33 in normal liver from both mice and human beings are the liver sinusoidal endothelial cells and, in fibrotic liver, the activated hepatic stellate cells (HSC). Moreover, IL-33 expression was increased in cultured HSC when stimulated by pro-inflammatory cytokines. In conclusion, IL-33 is strongly associated with fibrosis in chronic liver injury and activated HSC are a source of IL-33.

**Keywords:** IL-33 • ST2 • fibrosis • hepatic stellate cells • Th2 cytokines

### Introduction

Liver fibrosis is the main cause of organ failure in chronic liver disease. It can result from reiterated tissue damage due to infection (mostly hepatitis B virus [HBV] and hepatitis C virus [HCV]), toxic/drug exposure or metabolic or autoimmune disorders [1]. After two or three decades, patients become cirrhotic and are at high risk of developing hepatocellular carcinoma (HCC).

Liver fibrosis is due to the progressive accumulation of extracellular matrix (ECM) proteins in the liver sinusoids. During progression of hepatic fibrosis, sustained inflammation activates hepatic stellate cells (HSC), leading to their conversion into a fibrogenic and proliferative cell type. Activated HSC produce large amounts of collagen and thereby serve as the principal mediators of fibrogenesis

[2]. Chronic hepatitis that leads to fibrosis is characterized by a persistent inflammatory infiltrate and a Th2 polarized immune response. In contrast, Th1 cytokines generate a rapid and intense inflammatory response but cause little fibrosis. Thus, Th2 cytokines such as interleukin (IL)-6, IL-4 and IL-13 promote HSC proliferation, transforming growth factor (TGF)- $\beta$  synthesis and fibrogenesis [3].

IL-33, a pro-Th2 cytokine, is among the most recent cytokines to be identified. IL-33 belongs to the IL-1 family. It is also known as nuclear factor of high endothelial venules (NF-HEV) [4] and DVS 27 [5]. IL-33 is preferentially localized in the high endothelial venules of human tonsils, Peyer's patches and lymph nodes [4]. Recently, IL-33 has been observed by immunohistochemistry as constitutively expressed in the nucleus of endothelial cells from both small and large blood vessels of various tissues including human normal liver (NL) [6]. It is a dual-function protein that may act both as an intracellular nuclear factor and a cytokine. Indeed, IL-33 is an abundant chromatin-associated factor in the nucleus of endothelial cells exhibiting transcriptional repressor properties [7]. Interestingly, IL-33 has also been identified as the natural ligand for

\* Correspondence to: Dr. Michel SAMSON,  
EA 4427 SeRAIC / INSERM U.620, Université de Rennes 1,  
2 avenue du Prof. Léon Bernard 35043 Rennes cedex, France.  
Tel.: +33-02-23 23 48 06  
Fax: + 33-02-23 23 47 94  
E-mail: michel.samson@univ-rennes1.fr

ST2, an orphan membrane receptor [8]. In the presence of IL-33, ST2 binds IL-1RAcP and allows signalling through mitogen-activated protein kinases and NF- $\kappa$ B [8, 9]. Soluble IL-33 increases the secretion of Th2 cytokines (IL-4, IL-5 and IL-13) both *in vitro* and *in vivo* [8]. A recent study showed that IL-33 also reduces the development of atherosclerosis, a chronic inflammatory disease, through induction of IL-5 [10]. Heart failure and cardiac fibrosis are associated with the production of IL-33 from the cardiac fibroblasts [11]. The involvement of ST2 receptor was also investigated in human fibrotic diseases. Tajima *et al.* [12] showed that both ST2 and TGF- $\beta$  levels are increased in bleomycin-induced lung fibrosis. In a mouse model of hepatic fibrosis induced by CCl<sub>4</sub>, injection of the fusion protein ST2-Fc was shown to increase Th2 cytokine secretion and to enhance hepatic fibrosis [13].

Thus, given both the pro-Th2 activity of IL-33 and the crucial role of Th2 cytokines in the progression of liver chronic fibrosis, we investigated the presence of both IL-33 and its receptors in normal and CCl<sub>4</sub>-induced fibrotic mouse livers. We then analysed the production of IL-33 and its receptors in human healthy and fibrotic livers. Furthermore, we identified the cellular origin of IL-33 in liver and investigated the effect of pro-inflammatory cytokines on IL-33 expression by HSC.

## Materials and methods

### Mice

Seven-week-old female C57Bl/6 mice were treated with oral administration of CCl<sub>4</sub> (Sigma-Aldrich, St. Louis, MO, USA) diluted in olive oil. A first dose of 2.4 g/kg of mouse weight was administered to mice three days before starting weekly treatment with a 1.6 g/kg dose. After 12 weeks, mice were killed at 0, 4, 24, 48 and 72 hrs or 7 days after the last CCl<sub>4</sub> dose. Control mice were treated with the vehicle only. Fragments of mouse livers were fixed in 4% paraformaldehyde and embedded in paraffin or frozen in liquid nitrogen in the presence of the cryoprotectant isopentane. Serum aspartate aminotransferase (AST) and alanine aminotransferase (ALT) were measured according to the IFCC primary reference procedures and using the Olympus AU2700 Autoanalyser<sup>®</sup> (Olympus Optical Co. Ltd., Tokyo, Japan). All animals received humane care and all study protocols comply with the institution's guidelines.

### Human liver biopsies

Liver tissue samples were obtained from 34 patients with HCC undergoing surgical resection of the tumour as previously described [14]. Six histologically normal samples from metastatic colorectal cancer livers were used as controls. Access to this material was in line with French law and satisfied the requirements of the local Ethics Committee. Patients with HCC were 28 males and 6 females (59.3  $\pm$  9.9 years). The aetiology of fibrosis ( $n = 8$ ) and cirrhosis ( $n = 20$ ) included hepatitis C ( $n = 7$ ), hepatitis B ( $n = 7$ ) and alcohol abuse ( $n = 17$ ). Histological evaluation before their inclusion in the study ruled out the presence of tumour tissue in these samples. The histological stage of fibrosis was graded according to the

METAVIR score: F0 = no fibrosis, F1 = portal fibrosis without septa, F2 = portal fibrosis with few septa, F3 = numerous septa without cirrhosis, and F4 = cirrhosis. For each groups, number of patients were as follow: F0–F3:  $n = 8$  (F0:  $n = 3$ , F1:  $n = 3$ , F2:  $n = 1$ , F3:  $n = 1$ ) and F4:  $n = 20$ .

### RNA isolation and reverse transcription

Total RNA was extracted from human liver biopsies using guanidinium thiocyanate/cesium chloride and from mouse samples using TRIzol (Invitrogen, Carlsbad, CA). First-strand cDNA was produced using the SuperScript<sup>™</sup> II Reverse Transcriptase (Invitrogen). The SV Total RNA isolation Kit (Promega, Charbonnières-les-bains, France) and High-Capacity cDNA Archive Kit (Applied Biosystems, Foster City, CA, USA) were used for primary cells and cell lines.

### Real-time quantitative PCR (qPCR)

Real-time qPCR was performed using the fluorescent dye SYBR Green with the double-strand specific dye SYBR<sup>®</sup> Green system (Applied Biosystems) and the 7000 sequence detection system ABI Prism sequence detector (Applied Biosystems). Total cDNA (30 ng) was used as a template for amplification with the specific primer pair (Table 1) used at a 300 nM final concentration. Each measurement was performed in duplicate. 18S mRNA level was used as control and gene expression level was expressed relative to 18S mRNA.

### Cell culture

Human hepatic cells were isolated from histologically normal specimens from partial hepatectomy in patients undergoing hepatic resection for liver metastases. Hepatocytes, non-parenchymal cells (NPC) and activated HSC were isolated and cultured as previously described [15].

Hepatic cell lines, Hep3B and HepG2, were grown as recommended by American Type Culture Collection (Manassas, VA, USA). HepaRG cell line was grown as previously described [16]. Subcellular fractions were obtained using the TransFactor Extraction Kit (Clontech Laboratories, Mountain View, CA, USA). We analysed IL-33 protein after HSC stimulation with a pro-inflammatory cocktail containing 1 ng/ml IL-1 $\beta$ , 10 ng/ml IL-6, 20 ng/ml tumour necrosis factor (TNF)- $\alpha$  (R&D Systems, Minneapolis, MN, USA) and 100 ng/ml interferon (IFN)- $\gamma$  (BioSource Europe, Nivelles, Belgium) for 6 or 24 hrs, as indicated.

### Antibodies

See Table 2.

### Immunolocalization

Paraformaldehyde-fixed cryosections were permeabilized by 0.1% Triton X-100. HSC primary cultures were placed into flexiPERM chambers (Greiner Bio-One Kremsmünster, Austria), fixed with paraformaldehyde and permeabilized with 0.1% Triton X-100. 10<sup>5</sup> NPC were spotted on slides by Cytospin<sup>®</sup> (Shandon, Pittsburgh, PA, USA) and fixed using methanol/acetone.

**Table 1** Primers used

Gene	Forward	Reverse
Mouse IL-33	5'-ATGGGAAGAAGCTGATGGTG-3'	5'-CCGAGGACTTTTTGTGAAGG-3'
Mouse ST2	5'-ATTCAGGGGACCATCAAGTG-3'	5'-CGTCTTGAGGCTCTTTCTG-3'
Mouse IL-1RAcP	5'-TTGCCACCCAGATCTATTC-3'	5'-TGCAGGGAATAACCAGTTCC-3'
Mouse Collagen1A2	5'-AGGCTGACACGAAGTGAAGTA-3'	5'-ATGCACATCAATGTGGAGGA-3'
Mouse 18S	5'-CGCCGCTAGAGGTGAAATTC-3'	5'-TTGGCAAATGCTTTTCGCTC-3'
Human IL-33	5'-AATCAGGTGACGGTGTG-3'	5'-ACACTCCAGGATCAGTCTTG-3'
Human ST2	5'-CAACTGGACAGCACCTCTTG-3'	5'-AATCACCTGCGTCTCAGTC-3'
Human IL-1RAcP	5'-AAG AC AG CTGTTTC AATTC-3'	5'-TTGAAATTAAGGCAATGAGG-3'
Human 18S	5'-GTAACCCGTTGAACCCATT-3'	5'-CCATCCAATCGGTAGTAGCG-3'

PCR conditions: initial DNA denaturation (95°C, 10 min.), followed by 40 cycles of denaturation (95°C, 15 sec.), annealing and extension (60°C, 1 min.).

**Table 2** Antibodies used

Antibodies	Running concentrations	Manufacturers
Mouse monoclonal IgG1 anti-human IL-33 (clone Nussy-1)	1 µg/ml	
Polyclonal rabbit anti-human IL-33 (AT110)	10 µg/ml	Alexis Biochemicals (Lausen, Switzerland)
Polyclonal goat anti-mouse IL-33	5 µg/ml	R&D Systems (Minneapolis, MN)
Mouse monoclonal IgG2a anti-human α-SMA (Clone1A4)	0.35 µg/ml	
Mouse monoclonal IgG1 anti-human CD31 (clone JC70A)	1/10 <sup>e</sup>	
Mouse monoclonal IgG1 anti-human CD68 (clone KP1)	1/1 <sup>e</sup>	DakoCytomation (Glostrup, Denmark)
HRP-conjugated goat anti-mouse IgG	1 /200 <sup>e</sup>	
HRP-conjugated rabbit anti-goat IgG	1 /200 <sup>e</sup>	
Mouse monoclonal anti-human CD45 (IOL1c)	1/1 <sup>e</sup>	Immunotech (Marseille, France)
Cy5-conjugated bovine anti-goat IgG	1 /200 <sup>e</sup>	
Cy3-conjugated goat anti-rabbit IgG	1 /100 <sup>e</sup>	Jackson ImmunoResearch Europe (Suffolk, UK)
FITC-conjugated donkey anti-rabbit IgG	1 /200 <sup>e</sup>	
Mouse monoclonal IgG1 anti-human α-tubulin (clone B-5-1-2)	0.67 µg/ml	
Cy3-conjugated mouse monoclonal IgG2a anti-α-SMA (Clone1A4)	1 /100 <sup>e</sup>	Sigma-Aldrich (St. Louis, MO)
TRITC-conjugated goat anti-mouse IgG	1 /200 <sup>e</sup>	
Mouse monoclonal IgG2a anti-human Hsc70 (clone B6) polyclonal rabbit anti-human USF-1 (C-20)	0.1 µg/ml 0.25 liq/ml	Santa Cruz Biotechnology (Santa Cruz, CA)
FITC-conjugated mouse monoclonal IgG1 anti-human ST2L (clone B4E6)	10 µg/ml	MD Biosciences (Zürich, Switzerland)
Monoclonal rabbit anti-human CD3 (clone SP7)	1 /300 <sup>e</sup>	Thermo Fisher Scientific (Fremont, CA)

Endogenous peroxidase activity was inhibited with 3% H<sub>2</sub>O<sub>2</sub> and non-specific sites were blocked for 1 hr with 2% bovine serum albumin. Sections were incubated with the relevant primary antibody (as indicated in the figure legend) for 2 hrs at temperature and with goat antimouse immunoglobulins/horseradish peroxidase (HRP) secondary antibody for 1 hr at RT. The peroxidase reaction was developed using the Liquid DAB + Substrate Chromogen System (DakoCytomation, Glostrup, Denmark) or

β-amino-9-ethyl-carbazole (AEC; Vector Laboratories, Burlingame, CA) as substrate. Sections were finally counterstained with Mayer's haematoxylin. For immunofluorescence detection, fluorochrome-conjugated secondary antibodies were used for 1 hr at room temperature. Nuclei were counterstained with diaminobenzidine. Double stainings were performed by mixing the primary antibodies and mixing fluorochrome-conjugated reagents, respectively.

## IL-33 detection by Western blotting or ELISA

Cells were lysed in RIPA buffer (50 mM Tris-HCl pH 7.4; 1% Triton X-100; 25 mM HEPES; 150 mM NaCl; 0.2% deoxycholate; 5 mM MgCl<sub>2</sub>; 1 mM Na<sub>3</sub>VO<sub>4</sub>; 1 mM NaF). Proteins (30 µg) from each sample were separated in a 16% polyacrylamide gel and transferred onto a nitrocellulose membrane (Protran BA 83 Nitrocellulose; Whatman, Kent, UK). Membranes were incubated with monoclonal anti-human IL-33, anti-human  $\alpha$ -tubulin, anti-human Hsc70 or anti-human USF-1, and then with secondary goat antimouse immunoglobulins/HRP. Proteins were detected by enhanced chemiluminescence and LAS-3000 imager analysis (Fujifilm Europe, Düsseldorf, Deutschland).

For ELISA quantification, culture supernatants were collected after 24 hrs incubation with or without the cytokine cocktail. IL-33 was measured in these supernatants using the soluble human IL-33 detection set from Apotech (Lausen, Switzerland), according to the provider's instructions.

## Statistical analysis

The one-way ANOVA was performed then Student–Newman–Keuls multiple comparison test was used to test the significance of biological parameters measured in human samples. Alternatively, Student's t-test was used to analyse data obtained from fewer samples. The correlation between continuous variables was examined using Spearman's rank-order coefficients. For all statistical analyses, \* denotes  $P < 0.05$ , \*\* $P < 0.01$  and \*\*\* $P < 0.001$ .

## Results

### IL-33 is overexpressed in mouse liver fibrosis

Carbon tetrachloride-induced liver fibrosis model is a well-established model for studying liver inflammation and fibrosis [17, 18]. We measured levels of ALT and AST in blood samples from C57Bl/6 mice with CCl<sub>4</sub>-induced liver fibrosis after 12 weeks of treatment. Mouse hepatocytes were damaged by the treatment, as expected (Fig. 1A). We then measured the levels of mouse IL-33, ST2 and IL-1RAcP transcripts, using real-time qPCR, in the livers of treated mice before the 12th injection (0 hr) or at 4 hrs to seven days after the last CCl<sub>4</sub> ingestion. IL-33 mRNA levels were increased in fibrotic liver and were further enhanced 24 to 48 hrs after CCl<sub>4</sub> treatment. ST2 mRNA levels were also increased with a similar kinetic and IL-33 mRNA levels statistically correlated with ST2 mRNA levels (Spearman correlation:  $r = 0.632$ ;  $P < 0.001$ ) (Fig. 1B). In contrast, no significant change in IL-1RAcP expression was detected (Fig. 1B). We also noticed that the basal expression of collagen 1A2 mRNA is significantly increased after 12 weeks (0 hr) and 13 weeks (7 days) in CCl<sub>4</sub>-treated mice (Fig. 1C). Furthermore, collagen 1A2 mRNA levels were strongly induced 48 hrs after CCl<sub>4</sub> ingestion and collagen 1A2 mRNA levels statistically correlated with IL-33 mRNA levels (Spearman correlation:  $r = 0.811$ ;  $P < 0.001$ ).

As expected, CCl<sub>4</sub> treatment induced collagen deposition in mouse liver as shown by Sirius red staining of collagen on paraffin-embedded mouse liver sections (Fig. 2A). We studied IL-33 protein levels by immunohistochemistry in fibrotic livers (Fig. 2B). IL-33 protein was detected in vascular endothelial cells (Fig. 2Bb, g), in sinusoidal cells (Fig. 2Ba, b), in cells distributed along fibrous septa bridging portal tracts (Fig. 2Bc, f, h) and in immune infiltrates (Fig. 2Bb). No specific immunofluorescence was detected in appropriate controls (irrelevant primary antibody or when antimouse IL-33 was pre-absorbed with recombinant mouse IL-33) (Fig. 2Bd, e). To better characterize the cell type expressing IL-33 in fibrotic tissue, double staining with aniline blue revealed that some IL-33<sup>+</sup> cells were closely associated with type I collagen deposition (Fig. 3Aa, c). Furthermore, to validate the fact that activated HSC could be a source of IL-33 in fibrotic liver, we carried out immunofluorescence staining for  $\alpha$ -smooth muscle actin ( $\alpha$ -SMA), a specific marker of smooth muscle cells and activated HSC. Indeed when activated, HSC take up a myofibroblastic-like phenotype that is contractile because of the cytoskeleton reorganization and the formation of stress fibers containing  $\alpha$ -SMA in their cytoplasm [19]. We observed a colocalization of  $\alpha$ -SMA and IL-33 staining (Fig. 3B), indicating that activated HSC expressed IL-33 *in vivo*.

### IL-33 and ST2 mRNA levels are higher in human fibrotic and cirrhotic livers, but not in hepatocellular carcinoma, than in normal livers

To further investigate the relationship between IL-33 and fibrosis, we quantified the mRNA levels of IL-33 and its receptors, ST2 and IL-1RAcP, in human liver biopsies from NL, non-tumoral liver (NT) – corresponding to the fibrotic tissue surrounding the tumour – and HCC using real-time qPCR. IL-33 mRNA levels were significantly higher in the non-tumoral fibrotic livers than in either HCC or control liver. A similar pattern was observed for the mRNA levels of both IL-33 receptors, ST2 and IL-1RAcP (Fig. 4A).

Non-tumoral fibrotic livers were separated as a function of the severity of fibrosis, and identified as fibrosis (F0-F3) or cirrhosis (F4). IL-33 and ST2 are clearly associated with both fibrosis and cirrhosis (Fig. 4B). In contrast, IL-1RAcP mRNA levels did not significantly differ between the fibrotic liver groups. In conclusion, production of IL-33 and its receptor ST2 are linked to the fibrosis process.

### IL-33 and ST2 expression in human liver

To identify the cellular source of human IL-33, we determined its localization by immunohistochemistry in normal and fibrotic livers. Before, human tonsils sections were used as positive controls and IL-33 was found in the high endothelial cell venules of the T territory and had a nuclear localization (Fig. 5A), as previously described [4]. In fibrotic liver (Fig. 5B, C), IL-33 staining was

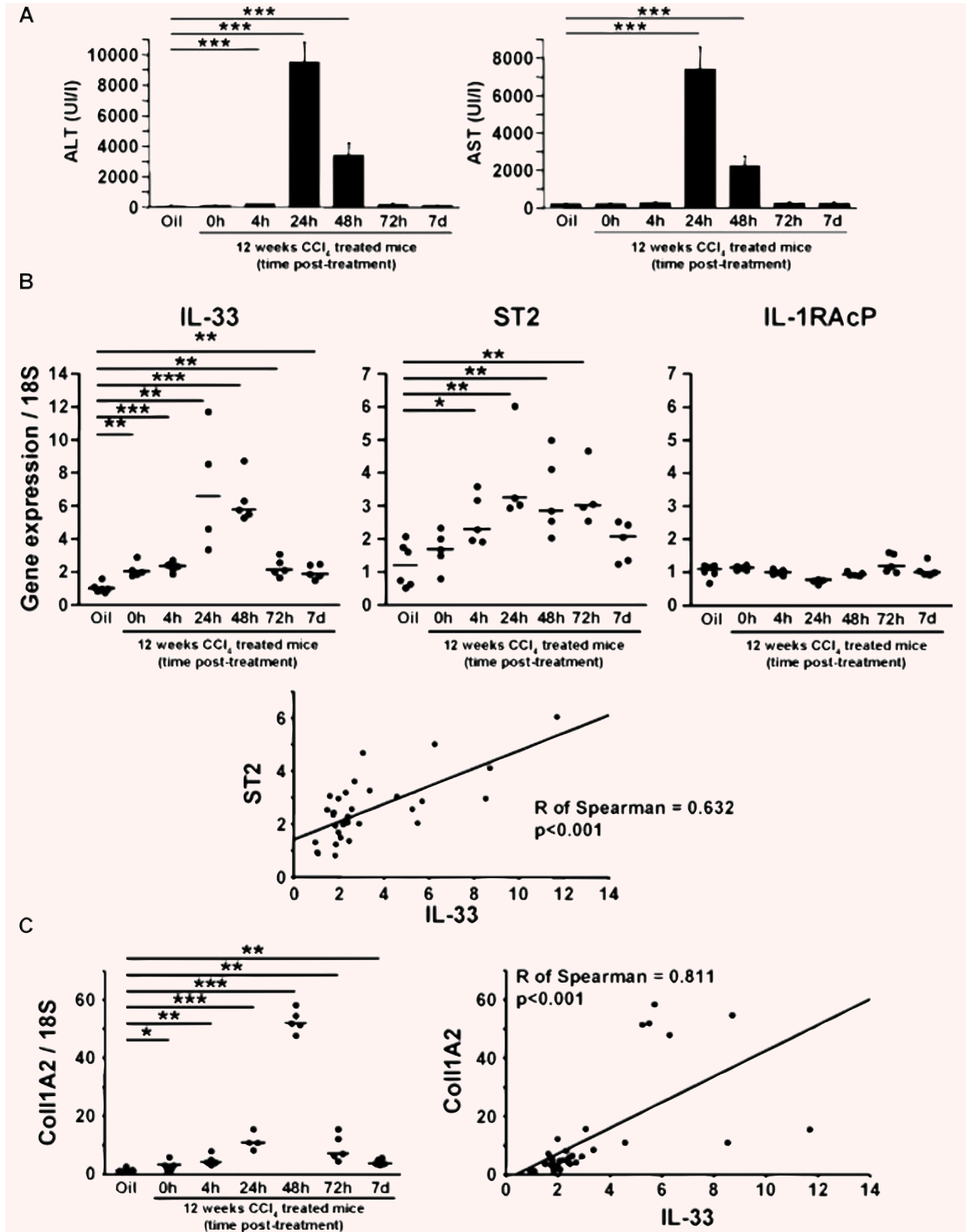




**Fig. 1** IL-33 mRNA is overexpressed in mouse liver fibrosis. (A) Blood levels of ALT and AST in C57Bl/6 mice treated for 12 weeks with CCl<sub>4</sub>. Real-time PCR analysis of mRNA levels of IL-33, ST2 and IL-1RAcP (B) and collagen 1A2 (C) in oil control (Oil) and livers from C57Bl/6 mice treated for 12 weeks with CCl<sub>4</sub> and killed 0, 4, 24, 48 and 72 hrs or 7 days after the last administration of CCl<sub>4</sub>. Expression levels for genes of interest are expressed as ratios relative to 18S levels. *P*-values for differences between populations were determined with Student's *t*-test (\**P* < 0.05; \*\**P* < 0.01; \*\*\**P* < 0.001). Graphic representation of the Spearman's rank correlation coefficient between IL-33 and ST2 (B) and between IL-33 and collagen 1A2 (C).

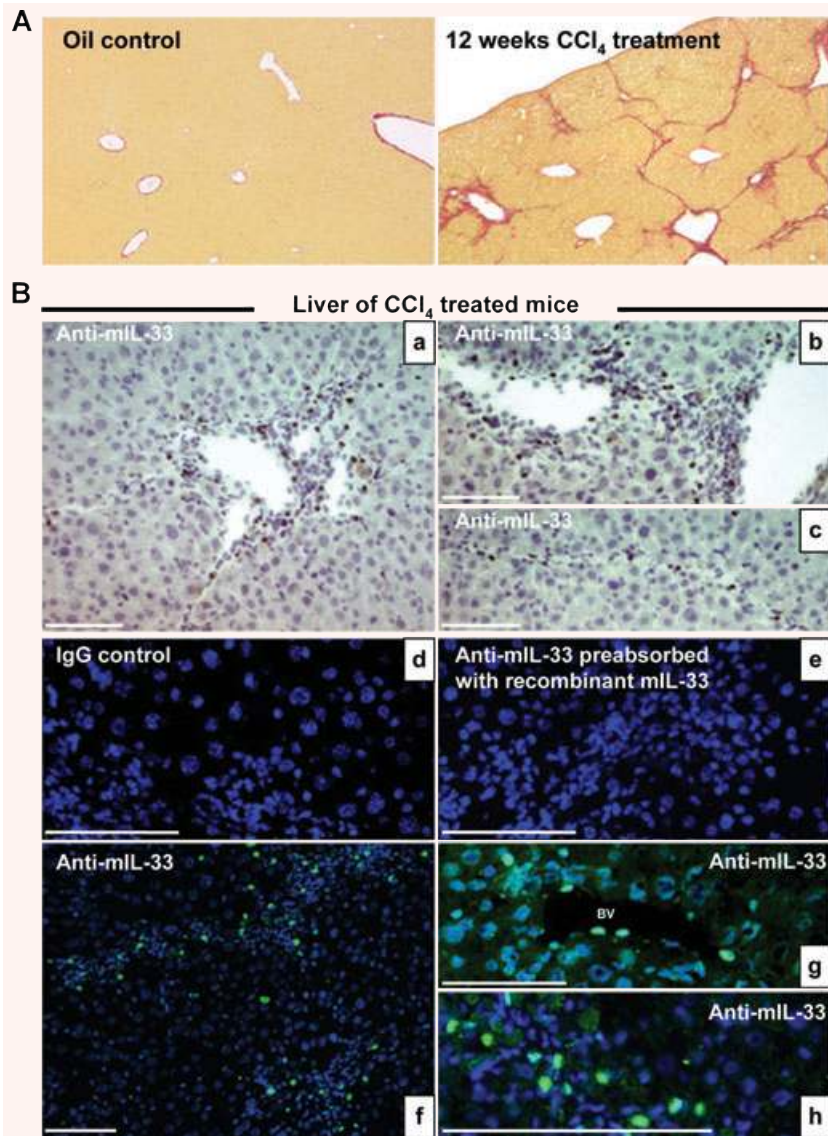
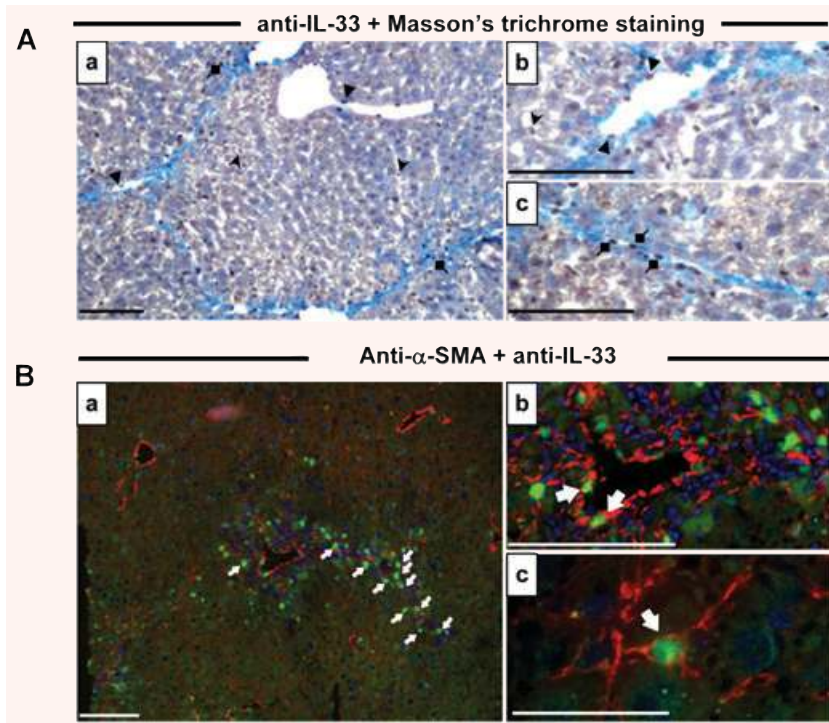


**Fig. 2** IL-33 distribution in mouse liver sections. (A) Photomicrographs of liver sections stained with Sirius red from mice treated for 12 weeks with CCl<sub>4</sub> (right) or oil (left). (B) Immunohistochemistry on frozen liver sections from oil- or CCl<sub>4</sub>-treated mice, killed 24 hrs after the last administration of CCl<sub>4</sub> as indicated, was performed with the non-specific IgG control, the antimouse IL-33 pre-absorbed with the recombinant mouse IL-33, the antimouse IL-33 antibody and fluoresceine iso thio cyanate conjugated secondary antibodies were used. Nuclei were counterstained with diaminobenzidine. Cells staining positive for IL-33 are indicated with full white arrows. BV: blood vessel; LSEC: liver sinusoidal endothelial cell. Scale bars represent 100 μm.

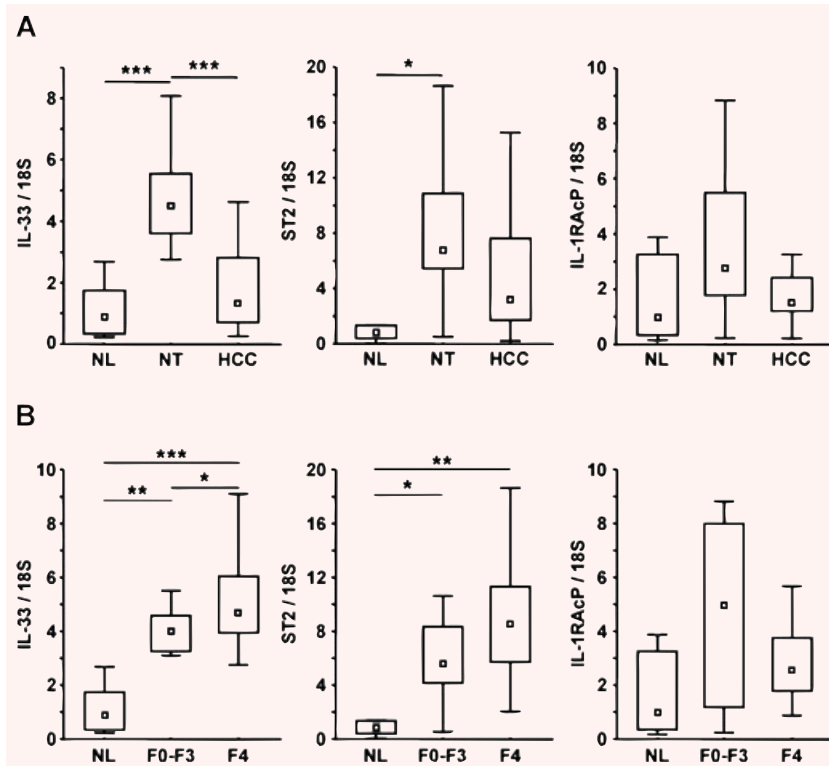
concentrated in endothelial cells from portal vessels (Fig. 5Ca) and in sinusoids (Fig. 5Cb), with a nuclear localization. No staining was detectable in hepatocytes or biliary ducts. Additional cells showed positive staining, in areas of inflammation and fibrous scars (Fig. 5Cc, d). As expected, α-SMA staining was much more intense in fibrotic liver than in NL (Fig. 6A) and was associated

with fibrous scars, where activated HSC produce collagen in excess. Serial sections immunolabelled with anti-IL-33 (Fig. 6Ba, c) and anti-α-SMA (Fig. 6Bb, d) revealed staining in the same areas for both proteins. The immunofluorescence staining confirms, as observed in mouse livers, the presence of double positive cells, α-SMA and IL-33, in fibrotic areas (Fig. 6C).

**Fig. 3** IL-33 co-localization with  $\alpha$ -SMA in mouse liver sections. **(A)** Immunohistochemistry on frozen liver sections from CCl<sub>4</sub>-treated mice, killed 24 hrs after the last administration of CCl<sub>4</sub>, was performed with the antimouse IL-33 antibody and counterstained according to the Masson's trichrome protocol **(A)** or co-localized with the Cy3- $\alpha$ -SMA antibody **(B)**. Cells staining positive for IL-33 are indicated with full arrows (endothelial cells), arrowheads (sinusoidal cells) and diamonds (fibrous scar cells). Scale bars represent: 40  $\mu$ m for **Bc**, 100  $\mu$ m for others.



**Fig. 4** IL-33 and ST2 are overexpressed in human fibrotic and cirrhotic liver. **(A)** Real-time qPCR analysis of IL-33, ST2 and IL-1RAcP mRNA levels in NL ( $n = 6$ ), NT ( $n = 28$ ) and HCC ( $n = 22$ ). **(B)** Real-time qPCR analysis of IL-33, ST2 and IL-1RAcP mRNA levels in NL ( $n = 6$ ) and in NT classified as fibrosis (F0-F3;  $n = 8$ ) or cirrhosis (F4;  $n = 20$ ). Results are expressed as ratios relative to 18S.  $P$ -values for differences between populations were determined with the Student–Newman–Keuls multiple comparison test ( $*P < 0.05$ ;  $**P < 0.01$ ;  $***P < 0.001$ ).



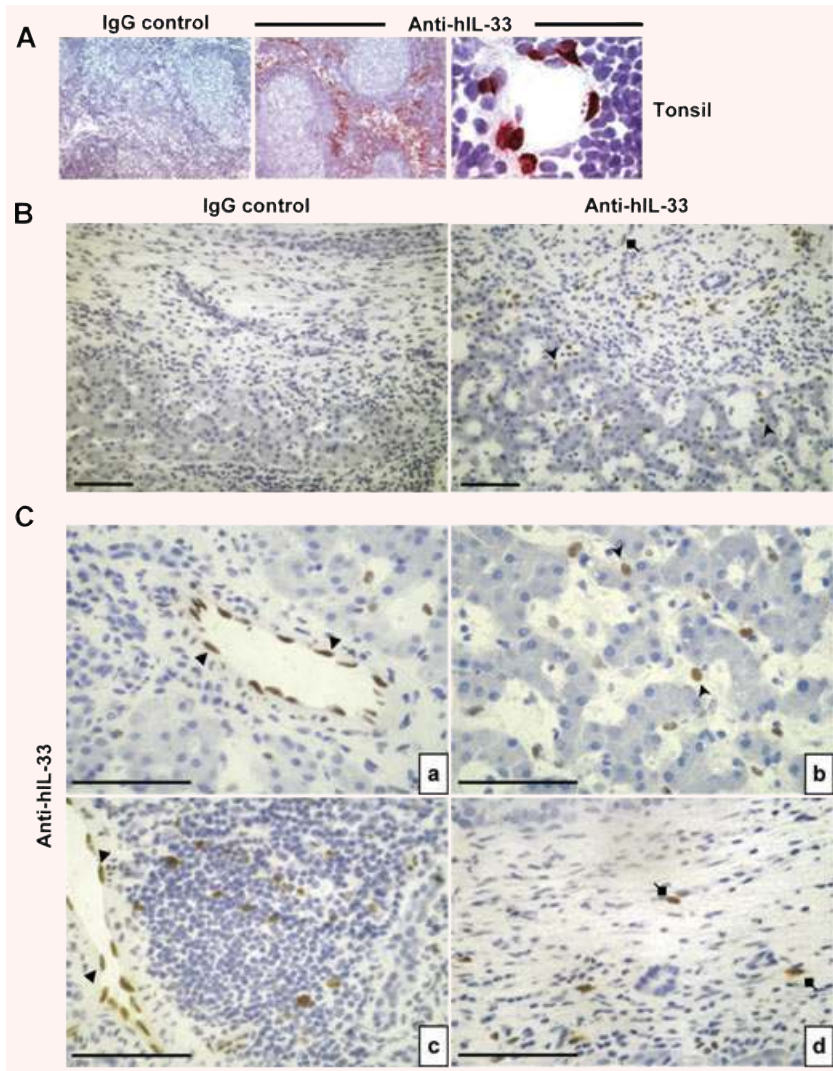


**Fig. 5** IL-33 distribution in human liver sections. Immunohistochemistry was performed with isotype controls or anti-IL-33 (Nessy-1) on frozen sections of human healthy tonsils (**A**) or of human livers (**B** and **C**). Cells staining positive for IL-33 are indicated with full arrows (endothelial cells), arrowheads (sinusoidal cells) and diamonds (fibrous scar cells). Scale bars represent 100  $\mu$ m.

Furthermore to identify the cellular target of human IL-33 in human fibrotic liver, we determined the localization of the specific IL-33 receptor, ST2 by immunohistochemistry in fibrotic liver sections. ST2 staining was associated with immune infiltrate (Fig. 7A), as well as was the pan-T lymphocyte marker, CD3 (Fig. 7B). Co-staining experiments revealed that ST2<sup>+</sup> cells are T lymphocytes (Fig. 7C).

### **Nuclear IL-33 is produced by sinusoidal endothelial cells in normal liver**

To elucidate IL-33 localization more precisely in NL, we studied IL-33 in various primary human hepatic cultures and cell lines. We found that NPC had higher levels of IL-33 transcripts than total liver, whereas no IL-33 mRNA was detected in hepatocytes (Fig. 8A). The presence of the IL-33 pro-form of 33 kD was confirmed by

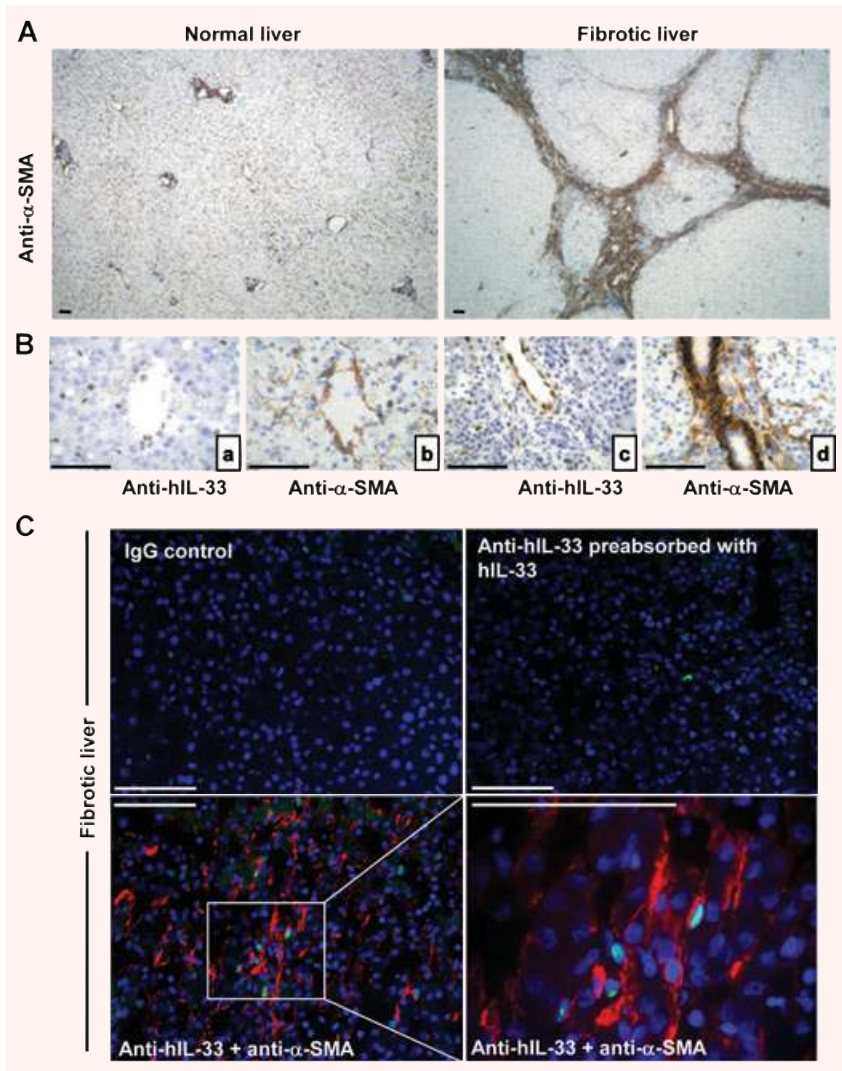
Western blot analysis in isolated NPC; IL-33 remained undetectable in primary hepatocytes and HCC cell lines (Fig. 8B). Using immunocytolocalization on freshly isolated NPC from NL, we determined which sinusoidal cell subpopulations were able to produce IL-33. Co-localization studies were performed using specific markers for endothelial cells (CD31), leucocytes (CD45) and macrophages and Kupffer cells (CD68) (Fig. 8C–f). 25% of the NPC were IL-33<sup>+</sup> and 87% of the IL-33<sup>+</sup> cells were also positive for CD31 (Fig. 8Cg). We did not detect IL-33 in leucocytes, macrophages or Kupffer cells (Fig. 8Ce, f).

### **Human culture-activated HSC expressed IL-33**

During fibrosis, quiescent HSC become activated and proliferate in the perisinusoidal space. The increase of IL-33 in fibrotic livers



**Fig. 6** IL-33 co-localization with  $\alpha$ -SMA in human liver sections. **(A)** Immunohistochemistry was performed with anti- $\alpha$ -SMA (clone 1A2) which stained the smooth muscle cells and activated HSC in human NL (left) and in fibrotic liver (right). **(B)** Serial sections of fibrotic livers were stained with anti-human IL-33 (Nessy-1) or anti- $\alpha$ -SMA. **(C)** Immunohistochemistry on frozen human fibrotic liver sections was performed with non-specific IgG, with anti-human IL-33 (Nessy-1) pre-absorbed with recombinant human IL-33 (Nessy-1), or with anti-human IL-33 antibody plus Cy3- $\alpha$ -SMA antibody. Nuclei were counterstained with diaminobenzidine. Scale bars represent 100  $\mu$ m.



could be explained by its production by activated HSC, as suggested by our immunolocalization studies in both mouse and human fibrotic livers. Thus, HSC were isolated from human livers and cultured. We measured IL-33 mRNA by real-time qPCR in culture-activated HSC and compared this to its level in total liver and in NPC (Fig. 9A). The detection of IL-33 *in situ* showed that IL-33 is nuclear. To confirm this subcellular localization of IL-33, cytosolic and nuclear fractions were prepared from culture-activated HSC. Western blot analysis showed that the IL-33 pro-form was mainly found in the nuclear fractions (Fig. 9B). Immunocytolocalization of IL-33 in culture-activated HSC (Fig. 9Cb, d) confirmed the presence of IL-33 in these cells and showed a nuclear subcellular localization.  $\alpha$ -SMA cytolocalization in activated (myo)fibroblastic HSC served as a positive control (Fig. 9Cc, d). These findings thus demonstrated that activated HSC produce the IL-33 pro-form.

### IL-33 is induced under pro-inflammatory conditions in culture-activated HSC

The modulation of IL-33 expression in growing HSC was studied in the presence of pro-inflammatory cytokines added alone or in combination. The greatest increase in IL-33 was observed after stimulation with a 'pro-inflammatory cytokine cocktail' containing TNF- $\alpha$ , IL-1 $\beta$ , IL-6 and IFN- $\gamma$ . As shown in Fig. 10, IL-33 mRNA was induced in activated HSC after 6 hrs exposure to the cytokine cocktail (Fig. 10A) and IL-33 protein was induced after 24 hrs exposure to this cocktail (Fig. 10B). We then examined the possibility for IL-33 to be released in the HSC conditioned media using ELISA. Indeed, IL-33 was detected after 24 hrs in control culture conditions at low levels, and when HSC were stimulated by the cytokine cocktail, soluble IL-33 levels were 15-fold increased (Fig. 10C).

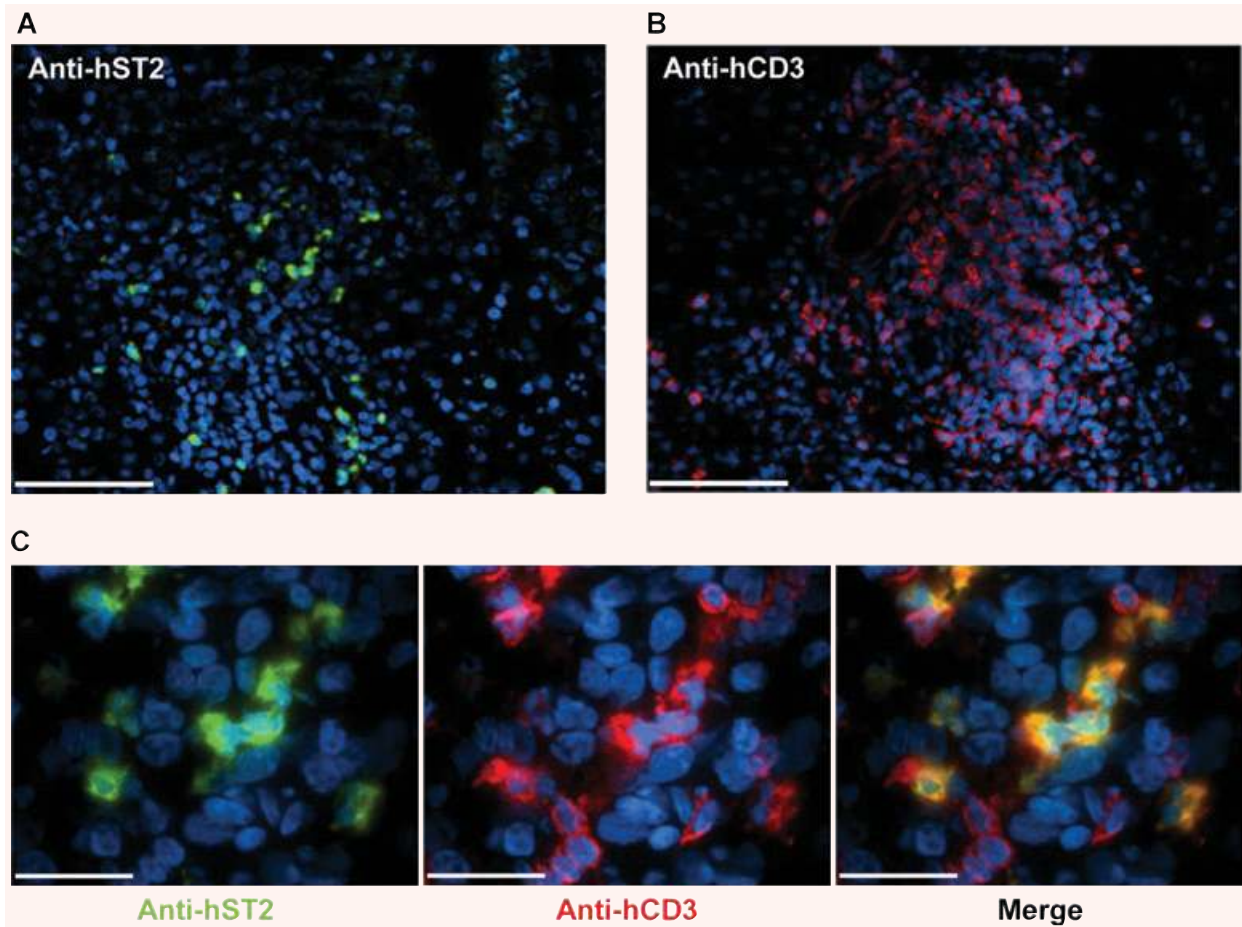


**Fig. 7** ST2 receptor co-localization with CD3 in human fibrotic liver sections. Immunohistochemistry on frozen human fibrotic liver sections was performed with fluoresceine iso thio cyanate labelled murine anti-human ST2 antibody (**A**, green) and with anti-CD3 antibody revealed with cyanin-3 labelled goat anti-rabbit IgG antibody (**B**, red). Scale bars represent 100  $\mu\text{m}$ . (**C**) Merged images illustrate co-localization of ST2 and CD3. Scale bars represent 40  $\mu\text{m}$ . For all pictures, nuclei were counterstained with diaminobenzidine.

## Discussion

The progression of chronic liver fibrosis towards advanced stage disease requires sustained inflammation. Th2 cytokines such as IL-4 and IL-13 are reported to be involved in the fibrotic process [3, 20, 21] and collagen synthesis [22, 23]. Recently a new pro-Th2 interleukin, named IL-33, was discovered. Recombinant IL-33 induces IL-5 and IL-13 production by CD4<sup>+</sup> T lymphocytes *in vitro* [8]. IL-33 is also involved in the induction of the Th2 response to intestinal helminth infection *in vivo* [8]. Moreover, injection of recombinant IL-33 into mice leads to enhanced levels of IL-13 in serum and increased expression of IL-4, IL-5 and IL-13 in liver [8]. Here, we demonstrate that expression of IL-33, and its receptors, ST2 and IL-1RAcP, are associated with both mouse and human liver fibrosis, but not with HCC. We observed

an increase in IL-33 and ST2 levels, while IL-1RAcP levels were not affected by the severity of fibrosis. Furthermore, we provided evidence that IL-33 levels are closely correlated to collagen synthesis in mouse and human livers during chronic injury. Our results are consistent with recent studies demonstrating that IL-33 production is associated with chronic inflammation in patients with rheumatoid arthritis and Crohn's disease [7] and in mice with cardiac fibrosis [11].

To identify the cellular source of IL-33 in normal and diseased livers, we carried out several immunohistochemical studies and immunolocalization in isolated hepatic cells. We demonstrated that IL-33 was present in vascular endothelial cells and sinusoidal cells in human liver. Moreover, analysis of a NPC-enriched population, including Kupffer cells, liver sinusoidal endothelial cells and quiescent stellate cells, showed that most IL-33<sup>+</sup> cells expressed CD31,

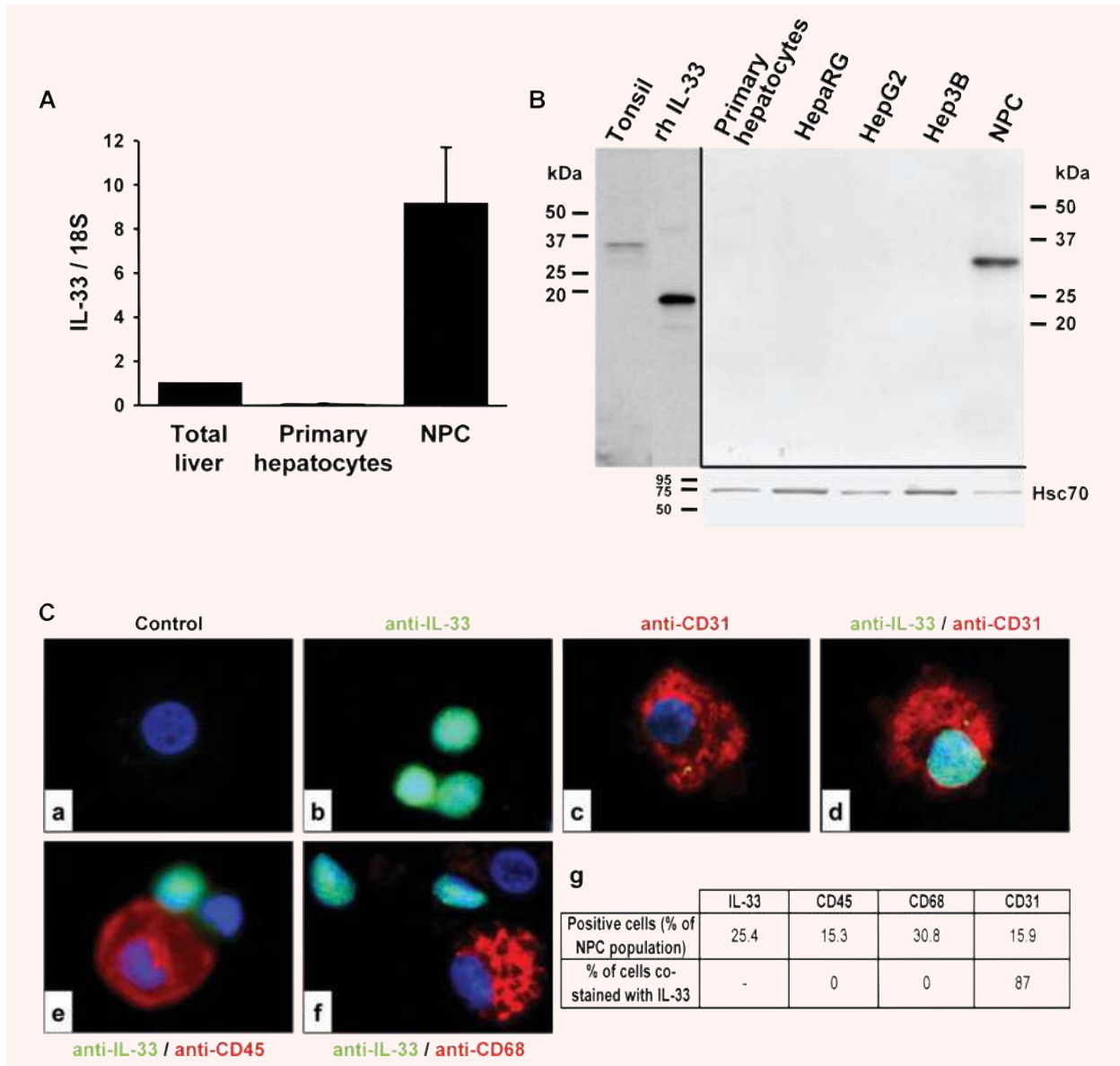


**Fig. 8** IL-33 pro-form is present in liver sinusoidal endothelial cells. **(A)** Real-time qPCR analysis of IL-33 mRNA levels in total NL, human primary cultured hepatocytes and in NPC. Results are expressed as ratios relative to 18S and are the average of three independent experiments. **(B)** Detection by Western blot of IL-33 in primary human hepatocytes, HepaRG, HepG2, Hep3B and NPC. **(C)** Immunocytochemistry was performed in liver NPC with anti-IL-33 (b, d, e, f; AT110; green) and anti-CD31 (c, d), anti-CD45 (e) or anti-CD68 (f) antibodies (red). Control experiment with IgG is shown (a). The table 'g' summarizes the percentage of cells that were positive for the different markers labelling the NPC spotted on slides by Cytospin<sup>®</sup>. More than 300 cells were counted per slides ( $n = 3$ ).

an endothelial cell marker. This strongly suggested that in NL, IL-33 is mainly produced by the liver sinusoidal endothelial cells. Similarly to NL, IL-33 was present in endothelial and sinusoidal cells of fibrotic liver. These observations are consistent with previous findings of IL-33 in endothelial cells of high endothelial venules

from human tonsils [4], and in endothelial cells from chronically inflamed tissues in rheumatoid arthritis and Crohn's disease [7]. Our findings also suggest that activated HSC produce IL-33 and that, in inflamed and fibrotic livers, IL-33-producing cells are located in fibrotic areas where such activated HSC produce collagen

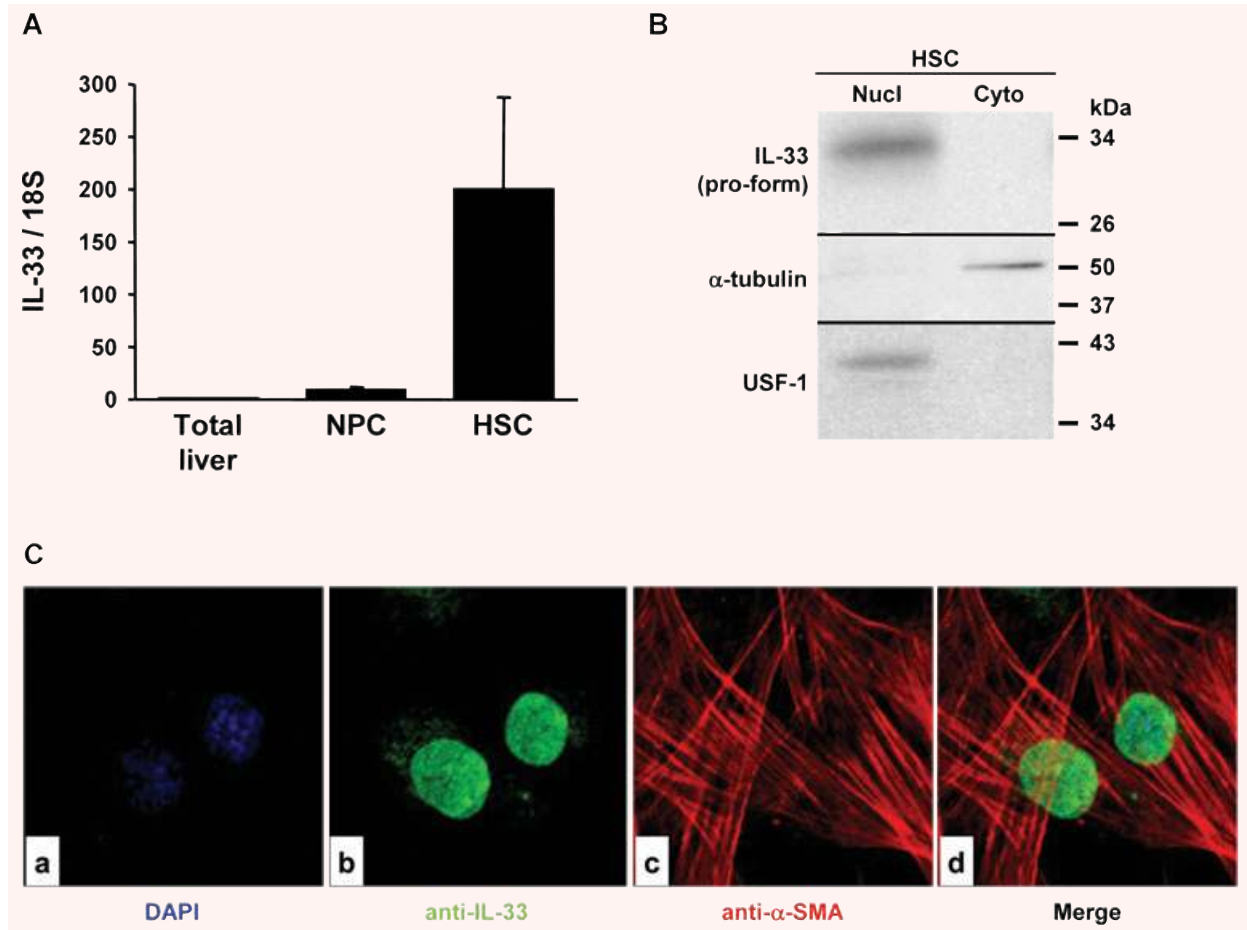


**Fig. 9** IL-33 is expressed by activated HSC. **(A)** Real-time qPCR analysis of IL-33 mRNA levels in total NL, NPC and culture-activated HSC. Results are expressed as ratios relative to 18S and are the average of three independent experiments. **(B)** Western blot of IL-33,  $\alpha$ -tubulin and USF-1 in nuclear (Nucl) and cytosolic (Cyto) subcellular fractions prepared from activated HSC. **(C)** Immunolocalization of IL-33 (b, d; AT110; green) and  $\alpha$ -SMA (c, d; red) in cultured HSC.

in excess. Previous studies have shown IL-33 to be constitutively produced in smooth muscle cells, activated dermal fibroblasts and cardiac fibroblasts [11]. It should be noted that these cell types, as with activated HSC, display common morphological and biochemical features of (myo)fibroblasts. Overall, our data suggest that endothelial cells and stellate cells constitute major sources of IL-33 in liver fibrosis and that the increase in IL-33 mRNA levels observed in liver fibrosis could be due to activation and proliferation of HSC or/and increased numbers of endothelial cells. Similarly to IL-1, IL-33 localizes to the nucleus [4, 6, 7, 24]. Our findings from both *in situ* immunolocalization and subcellular fraction analysis confirmed that IL-33 was present in the nuclei of liver endothelial cells and activated HSC. The inflammatory response is critical for fibrogenesis and cytokine secretion by leucocyte infiltrates or by hepatic cells themselves, and regulate the progression of fibrosis. Little is yet known about the regulation of IL-33; how-

ever, IL-1 $\alpha$ , IL-1 $\beta$ , IFN- $\gamma$  and TNF- $\alpha$  have been reported to increase IL-33 expression [5, 8]. Here, we showed that a pro-inflammatory cytokine cocktail, containing IL-6, TNF- $\alpha$ , IFN- $\gamma$  and IL-1 $\beta$ , increased both mRNA and protein levels of IL-33 in HSC.

Finally, as we observed an increase of mRNA levels of IL-33 receptor, ST2, associated with the severity of fibrosis, we carried out immunohistochemical studies to identify the cellular target of IL-33 in liver. We showed that ST2<sup>+</sup> cells were well present in human fibrotic livers and were T lymphocytes [25]. Th2 lymphocytes constitute target cells for soluble IL-33 and crucial immune regulatory cells for fibrosis development [3, 8, 20, 21]. Therefore, IL-33 that can be produced as a soluble cytokine by activated HSC in fibrotic liver may stimulate pro-fibrogenic Th2 cytokines by T lymphocytes.

In conclusion, we provide evidence suggesting the strong association between the expression of IL-33 and its specific receptor ST2, and the development of liver fibrosis.

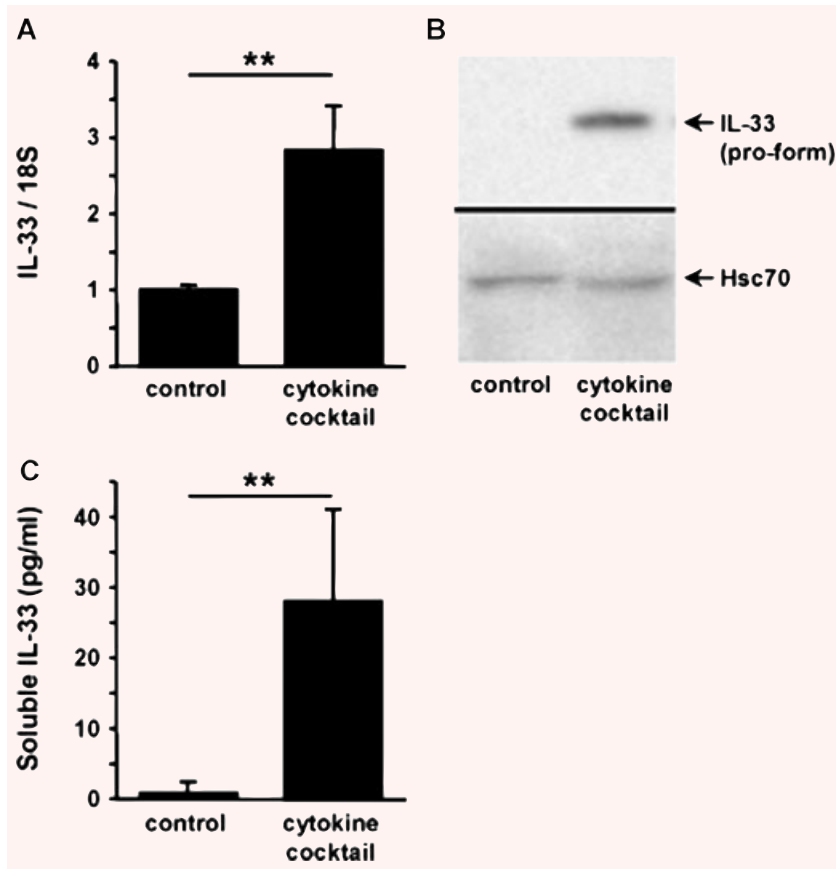


**Fig. 10** IL-33 in HSC is increased by pro-inflammatory cytokine stimulation. **(A)** Real-time qPCR analysis of IL-33 mRNA levels in activated human HSC stimulated for 6 hrs with a cytokine cocktail (IL-1 $\beta$ , IL-6, TNF- $\alpha$  and IFN- $\gamma$ ). Results are expressed as ratios relative to 18S and are the average of three experiments. Detection of intracellular IL-33 pro-form by Western blot **(B)** or of soluble IL-33 in the conditioned media by ELISA **(C)** was performed in activated HSC stimulated for 24 hrs with the cytokine cocktail. Results are the average of three independent experiments (\*\* $P < 0.01$ ).

## Acknowledgements

We are grateful Professor Yves Deugnier (Centre de Ressources Biologiques de Rennes) and Dr. Sylvie Caulet-Maugendre (Service d'anatomo-pathologie, CHU de Rennes) for their helpful cooperation. We thank Dr. Catherine Lucas (service Biochimie, CHU Rennes) for support in enzyme measurement in sera. We also thank Pascale Bellaud of IFR140

histology facilities. We thank Ouest-Genopole® 'Imagerie- Puce à cellules' facilities. P.M. was supported by a Ph.D. fellowship from the 'ministere de la recherche et de l'enseignement superieur'. This work was supported by INSERM, the 'ministere de la recherche et de l'enseignement superieur', the 'ligue nationale contre le cancer', the 'region Bretagne' the 'agence nationale de recherche sur le SIDA' and the 'societe nationale française de gastroenterologie'. The authors declare no conflict of interests.

## References

1. Friedman SL. Liver fibrosis – from bench to bedside. *J Hepatol.* 2003; 38: S38–53.
2. Gressner AM, Weiskirchen R. Modern pathogenetic concepts of liver fibrosis suggest stellate cells and TGF- $\beta$  as major players and therapeutic targets. *J Cell Mol Med.* 2006; 10: 76–99.
3. Wynn TA. Fibrotic disease and the T(H)1/T(H)2 paradigm. *Nat Rev Immunol.* 2004; 4: 583–94.
4. Baekkevold ES, Roussigne M, Yamanaka T *et al.* Molecular characterization of NF-HEV, a nuclear factor preferentially expressed in human high endothelial venules. *Am J Pathol.* 2003; 163: 69–79.
5. Onda H, Kasuya H, Takakura K *et al.* Identification of genes differentially expressed in canine vasospastic cerebral arteries after subarachnoid hemorrhage. *J Cereb Blood Flow Metab.* 1999; 19: 1279–88.
6. Moussion C, Ortega N, Girard JP. The IL-1-like cytokine IL-33 is constitutively expressed in the nucleus of endothelial cells and epithelial cells in vivo: a novel 'alarmin'? *PLoS ONE.* 2008; 3: e3331.
7. Carriere V, Roussel L, Ortega N *et al.* IL-33, the IL-1-like cytokine ligand for ST2 receptor, is a chromatin-associated nuclear factor in vivo. *Proc Natl Acad Sci USA.* 2007; 104: 282–7.
8. Schmitz J, Owyang A, Oldham E *et al.* IL-33, an interleukin-1-like cytokine that signals via the IL-1 receptor-related protein ST2 and induces T helper type 2-associated cytokines. *Immunity.* 2005; 23: 479–90.
9. Chackerian AA, Oldham ER, Murphy EE *et al.* IL-1 receptor accessory protein and

- ST2 comprise the IL-33 receptor complex. *J Immunol.* 2007; 179: 2551–5.
10. **Miller AM, Xu D, Asquith DL et al.** IL-33 reduces the development of atherosclerosis. *J Exp Med.* 2008; 205: 339–46.
  11. **Sanada S, Hakuno D, Higgins LJ et al.** IL-33 and ST2 comprise a critical biomechanically induced and cardioprotective signaling system. *J Clin Invest.* 2007; 117: 1538–49.
  12. **Tajima S, Bando M, Ohno S et al.** ST2 gene induced by type 2 helper T cell (Th2) and proinflammatory cytokine stimuli may modulate lung injury and fibrosis. *Exp Lung Res.* 2007; 33: 81–97.
  13. **Amatucci A, Novobrantseva T, Gilbride K et al.** Recombinant ST2 boosts hepatic Th2 response in vivo. *J Leukoc Biol.* 2007; 82: 124–32.
  14. **Theret N, Musso O, Turlin B et al.** Increased extracellular matrix remodeling is associated with tumor progression in human hepatocellular carcinomas. *Hepatology.* 2001; 34: 82–8.
  15. **Le Pabic H, Bonnier D, Wewer UM et al.** ADAM12 in human liver cancers: TGF-beta-regulated expression in stellate cells is associated with matrix remodeling. *Hepatology.* 2003; 37: 1056–66.
  16. **Gripon P, Rumin S, Urban S et al.** Infection of a human hepatoma cell line by hepatitis B virus. *Proc Natl Acad Sci USA.* 2002; 99: 15655–60.
  17. **Chang ML, Yeh CT, Chang PY et al.** Comparison of murine cirrhosis models induced by hepatotoxin administration and common bile duct ligation. *World J Gastroenterol.* 2005; 11: 4167–72.
  18. **Constandinou C, Henderson N, Iredale JP.** Modeling liver fibrosis in rodents. *Methods Mol Med.* 2005; 117: 237–50.
  19. **Cassiman D, Libbrecht L, Desmet V et al.** Hepatic stellate cell/myofibroblast subpopulations in fibrotic human and rat livers. *J Hepatol.* 2002; 36: 200–9.
  20. **Doucet C, Brouty-Boye D, Pottin-Clemenceau C et al.** Interleukin (IL) 4 and IL-13 act on human lung fibroblasts. Implication in asthma. *J Clin Invest.* 1998; 101: 2129–39.
  21. **Kaviratne M, Hesse M, Leusink M et al.** IL-13 activates a mechanism of tissue fibrosis that is completely TGF-beta independent. *J Immunol.* 2004; 173: 4020–9.
  22. **Tiggelman AM, Boers W, Linthorst C et al.** Collagen synthesis by human liver (myo)fibroblasts in culture: evidence for a regulatory role of IL-1 beta, IL-4, TGF beta and IFN gamma. *J Hepatol.* 1995; 23: 307–17.
  23. **Sugimoto R, Enjoji M, Nakamuta M et al.** Effect of IL-4 and IL-13 on collagen production in cultured L190 human hepatic stellate cells. *Liver Int.* 2005; 25: 420–8.
  24. **Werman A, Werman-Venkert R, White R et al.** The precursor form of IL-1alpha is an intracrine proinflammatory activator of transcription. *Proc Natl Acad Sci USA.* 2004; 101: 2434–9.
  25. **Coyle AJ, Lloyd C, Tian J et al.** Crucial role of the interleukin 1 receptor family member T1/ST2 in T helper cell type 2-mediated lung mucosal immune responses. *J Exp Med.* 1999; 190: 895–902.